Ind. J. Pharm. Edu. Res., 2026; 60:10.5530/ijper.20262558.
https://www.ijper.org

Original Article

N-Acetylcysteine in Pneumonia: Modulatory Effects on Pulmonary Inflammation and Alveolar Epithelial Cell Ferroptosis

Xiuxiu Zhao[1], Xueju Wang[2], Tianxiu Zhao[1,*]

[1]Department of Pediatrics, Weifang Second People's Hospital, Weifang, Shandong, CHINA.
[2]Department of Pediatrics, Sunshine Union Hospital, Weifang, Shandong, CHINA.

ABSTRACT

Objectives: Ferroptosis, an iron-dependent cell death pathway driven by lipid peroxidation, exacerbates alveolar epithelial damage in pneumonia. As a glutathione precursor, N-Acetylcysteine (NAC) may modulate this process through the Glutathione Peroxidase 4 (GPX4)/ Glutathione (GSH) axis. This study aimed to elucidate the protective mechanisms of NAC against alveolar epithelial cell injury and ferroptosis progression in a rat model of pneumonia, thereby establishing a scientific foundation for its potential clinical application. **Materials and Methods:** A dual-model approach was employed: (1) an *in vivoKlebsiella pneumoniae*-induced pneumonia model in Sprague-Dawley rats (n=25, randomized into 5 experimental groups), and (2) an *in vitro* Lipopolysaccharide (LPS)-stimulated inflammatory model using A549 alveolar epithelial cells. NAC was administered at varying concentrations for therapeutic intervention. Inflammatory cells (Eosinophils [EOS], Lymphocytes [LYM], and Neutrophils [NEU]) and cytokine levels (TNF-α, IL-1β, and IL-6) in Bronchoalveolar Lavage Fluid (BALF) were measured, and pathological lung tissue damage was observed. Cellular functional assays (EdU assay for proliferation, wound healing assay for migration, and flow cytometry for apoptosis), as well as molecular profiling of ferroptosis-related proteins (GPX4, SLC7A11, and ACSL4) via Western blot, were also carried out. **Results:** NAC administration significantly reduced inflammatory cell infiltration and cytokine levels in the BALF of Klebsiella pneumoniae-induced pneumonia rats (p<0.05), with the high-dose group (150 mg/kg) showing the most pronounced effect. Histomorphological analyses revealed alleviated alveolar structural damage in NAC-treated animals. In the cell model, NAC restored LPS-inhibited cell proliferation and migration, reduced apoptosis (p<0.05), and decreased TNF-α, IL-1β, and IL-6 levels in the culture medium. Mechanistically, NAC orchestrated a coordinated regulation of ferroptosis effectors, upregulating cytoprotective SLC7A11 and GPX4 while downmodulating pro-ferroptotic ACSL4, TFR1, and p53. This protective signature was associated with NRF2 pathway activation. **Conclusion:** NAC attenuated pneumonia injury through tripartite effects: suppressing inflammatory cascades, restoring alveolar barrier integrity, and inhibiting ferroptosis execution. These results delineate NAC's ferroptosis-targeted mechanism for pneumonia management.

Keywords: Alveolar Epithelial Cells, Ferroptosis, Inflammatory Response, N-acetylcysteine, Pneumonia.

Correspondence:
Dr. Tianxiu Zhao
Department of Pediatrics, Weifang Second People's Hospital, No. 7 Xueyuan Street, Kuiwen, Weifang, Shandong-261000, CHINA.
Email: 18765608169@163.com

Received: 04-05-2026;
Revised: 15-06-2026;
Accepted: 31-08-2026.

INTRODUCTION

Pneumonia primarily results from bacterial (e.g., Streptococcus pneumoniae, Klebsiella pneumoniae) or viral pathogens (e.g., influenza, Respiratory syncytial virus), with *K. pneumoniae* accounting for 11-17% of hospital-acquired cases globally.[1] Pneumonia remains the foremost cause of respiratory mortality after lung cancer, posing a significant health burden across all demographics.[2] A comprehensive 2020 epidemiological investigation conducted by Sun *et al.* including 1.42 million pneumonia cases throughout 23 Chinese provinces identified that children under five years of age represented a striking 65.8% of total reported cases.[3] Mounting evidence from international surveillance studies has documented a concerning upward trajectory in global pneumonia incidence in recent years.[4,5] While contemporary antibiotic regimens and anti-inflammatory interventions have markedly improved clinical outcomes, the escalating threat of antimicrobial resistance and irreversible pulmonary parenchymal damage continue to complicate therapeutic management. This persistent clinical conundrum has galvanized scientific consensus that elucidating the fundamental

DOI: 10.5530/ijper.20262558

Copyright Information :
Copyright Author (s) 2026 Distributed under Creative Commons CC-BY 4.0

Publishing Partner : Manuscript Technomedia. [www.mstechnomedia.com]

IN PRESS

pathophysiological mechanisms underlying pneumonia is paramount for pioneering effective treatment modalities.[6] The recent identification of ferroptosis-a distinct iron-dependent programmed cell death pathway-has emerged as a transformative concept in respiratory pathophysiology.[7] This unique cell death modality, characterized by lipid peroxidation accumulation and iron homeostasis disruption, has been mechanistically implicated in alveolar epithelial barrier compromise across multiple acute lung injury paradigms.[8] In pneumonia, pathogen-derived Lipopolysaccharide (LPS) activates Toll-Like Receptor 4 (TLR4)/Nuclear Factor Kappa-B (NF-κB) signaling, inducing iron overload via hepcidin suppression and Reactive Oxygen Species (ROS)-mediated lipid peroxidation. This cascade culminates in Acyl-CoA synthetase long-chain family member 4 (ACSL4)-dependent membrane rupture characteristic of ferroptosis.[9] Substantiating this pathogenic link, the work by Shen *et al.*, revealed a pronounced elevation of Malondialdehyde (MDA), a lipid peroxidation marker, in murine pneumonia models, concomitant with dramatic suppression of the iron metabolism-related gene Ferritin Heavy Chain-1 (FTH1).[10] In the study of Guo *et al.*, they found that ferroptosis inhibitor could effectively reverse idiopathic pulmonary fibrosis.[11] These findings suggest that ferroptosis may contribute to progressive pulmonary damage in pneumonia.

N-Acetylcysteine (NAC), a well-established mucolytic agent and glutathione precursor, has demonstrated clinically validated antioxidant properties in the treatment of Chronic Obstructive Pulmonary Disease (COPD).[12] At the same time, NAC has also been proved to have excellent effects on pulmonary fibrosis.[13] In pneumonia, the therapeutic effect of NAC has also been confirmed clinically.[14] Emerging evidence indicates that NAC's therapeutic potential extends beyond direct Reactive Oxygen Species (ROS) scavenging to include modulation of ferroptosis-through the Glutathione Peroxidase 4 (GPX4)/Glutathione (GSH) axis.[15] Notably, the functional activity of GPX4, a central regulator of ferroptosis, is critically dependent on the glutathione reductase system. As a cysteine donor, NAC may influence the ferroptosis signaling network at post-transcriptional levels by maintaining intracellular cysteine pool homeostasis.[16] Despite these advances, a critical knowledge gap remains regarding NAC's potential role in mitigating pneumonia-induced alveolar epithelial injury through targeted ferroptosis inhibition.

Based on current findings, we hypothesized that NAC mitigates alveolar epithelial damage by inhibiting ferroptosis via GPX4/SLC7A11 axis activation. To rigorously evaluate this hypothesis, we designed an integrated experimental approach employing a well-characterized rat pneumonia model, with the ultimate goal of establishing a theoretical foundation for ferroptosis-targeted pulmonary protection strategies.

MATERIALS AND METHODS

Experimental Animals

Male Sprague-Dawley rats (6-8 weeks old, 180-220 g) were obtained from Beijing Sinogenetic Biotechnology Co., Ltd., (Animal Use License No. SYXK [Jing] 2022-0024). The rats were housed under Specific Pathogen-Free (SPF) conditions at 18-26°C with 40-70% humidity and a 12 hr light/dark cycle, with five animals per cage. All experimental procedures were approved by the Animal Ethics Committee of Weifang Second People's Hospital (NO. 2025030303).

Grouping and Modeling

Following a one-week acclimatization period, the rats were randomly divided into five groups (n=5 per group). Single intratracheal instillation of 0.3 mL (1×10^9 CFU/mL) K. pneumoniae suspension.[17] Successful model establishment was confirmed after 7 days by characteristic symptoms including reduced food intake, increased mucopurulent nasal discharge, dyspnea, and pulmonary rales. The remaining group received an equivalent volume of sterile saline as the control group. The four pneumonia model groups were then subdivided into model group (no treatment), low-dose NAC group (50 mg/kg/day), medium-dose NAC group (100 mg/kg/day), and high-dose NAC group (150 mg/kg/day). NAC injections (H20051788, Hangzhou Minsheng Pharmaceutical Co., Ltd.,) were administered intravenously once daily for 7 consecutive days. Both the model and control groups received equivalent volumes of normal saline via intravenous injection once daily for 7 days.

Assessment of Pulmonary Inflammatory Response

Following completion of the treatment protocols, rats were humanely euthanized [Euthanasia via intraperitoneal pentobarbital (100 mg/kg) followed by cervical dislocation] and left lung tissues were aseptically excised. After three consecutive washes, Bronchoalveolar Lavage Fluid (BALF) was collected and centrifuged at 2500 rpm for 10 min to obtain supernatant for cytokine analysis. Tumor Necrosis Factor (TNF)-α (Shanghai Jianglai Biotechnology Co., Ltd., 1531619600), interleukin (IL)-1β (Shanghai Jianglai Biotechnology Co., Ltd., KB10760), and IL-6 (Shanghai Jianglai Biotechnology Co., Ltd., 1530960905) concentrations were quantified using Enzyme-Linked Immunosorbent Assay (ELISA) kits according to manufacturers' protocols. The precipitate was resuspended and evenly smeared on the center of microscope slides. After air-drying, Wright-Giemsa staining (Shanghai Beyotime Biotechnology, C0131) was performed, followed by differential cell counting (Eosinophils [EOS], Lymphocytes [LYM], and Neutrophils [NEU]) across five randomly selected high-power fields per sample.

IN PRESS

Histopathological Evaluation

Lung tissues were fixed with 4% paraformaldehyde, routinely embedded in paraffin, and sectioned. After dewaxing and hydration, Hematoxylin-Eosin (H&E) staining (Shanghai Beyotime Biotechnology, C0105S) was performed, followed by xylene clearing and mounting with a resinous medium. The pathological damage of lung tissue was observed under a microscope.

Cell Data

Human alveolar epithelial A549 cells (BeNa Culture Collection, BNCC337696) were maintained in a supporting medium supplemented with 10% Fetal Bovine Serum (FBS) and 1% penicillin-streptomycin at 37°C in a humidified 5% CO_2 incubator. The culture medium was refreshed every 48-72 hr, and cells were subcultured when reaching 80% confluence. Only cells in the logarithmic growth phase were utilized for experimental procedures.

Cell Grouping and Modeling

Cells were divided into a blank control group, a model group, and an NAC group. The blank control group was cultured normally without treatment. An *in vitro* inflammation model was established in both the model group and the NAC group by exposing cells to 10 μg/mL LPS (Merck, L5418) for 24 hr.[18] Subsequently, the NAC group received intervention with NAC at graded concentrations (0.5, 1, 2, 4, and 8 μmol/L). Cell viability was assessed using CCK-8 assays, and the optimal therapeutic NAC concentration was determined based on Half-Maximal Inhibitory Concentration (IC_{50}) calculations.

Cell Proliferation Assessment

Following interventions, cell proliferation was quantified using EdU assays (Guangzhou Ruibo Biotechnology Co., Ltd., C10310-1) per the manufacturer's protocol. After mounting, 3 random fields were photographed under a fluorescence microscope, and images were processed by Image-J software.

Cell proliferation rate=EdU positive cells/total cells × 100%

Migration Capacity Analysis

Cells from each group were mechanically wounded using sterile 200 μL pipette tips (time=0 hr). After 24 hr of culture, the scratch width was measured again.

Migration rate = (Initial width (0 hr) - Final width (24 hr))/Initial width] × 100%

Apoptosis Detection

Cells were digested with trypsin, centrifuged (1000 rpm/min) for 5 min, and adjusted to 1×10^8/mL. A 100 μL aliquot of cell suspension was stained with 5 μL Annexin V-FITC and 5 μL Propidium Iodide (PI) (Elabscience Biotechnology Co., Ltd., E-CK-A211) for 15 min in the dark. After adding 400 μL pre-cooled binding buffer, samples were analyzed by flow cytometry within 1 hr. Apoptosis rates were quantified using FlowJo software.

Inflammatory Cytokine Measurement

Culture supernatants were collected from each group and centrifuged at 2,000 × g for 10 min. TNF-α, IL-1β, and IL-6 concentrations in the supernatant were determined using ELISA kits according to the manufacturer's protocols.

Detection of Ferroptosis-related Proteins

Following cell lysis on ice, the lysate was centrifuged to collect the supernatant. Protein samples (20 μg per well) were separated by sodium dodecyl Sulfate-Polyacrylamide Gel Electrophoresis (SDS-PAGE) and subsequently transferred onto a polyvinylidene fluoride (PVDF) membrane. The membrane was blocked with 5% non-fat milk for 2 hr at room temperature, followed by overnight incubation at 4°C with primary antibodies against GPX4, ACSL4 (ab155282), SLC7A11 (ab307601), p53 (ab32509), TFR1 (ab109259), and GAPDH (ab8245) (1:1000 dilution, Abcam). After TBST washes, the membrane was incubated with an alkaline phosphatase-conjugated secondary antibody (1:2000 dilution) for 2 hr. Following liquid removal and additional washes, protein bands were visualized using a gel imaging system. GAPDH served as the loading control, and relative protein expression levels were quantified using ImageJ software.

Statistical Analysis

Statistical analyses were performed using SPSS 26.0. Continuous variables are presented as mean±standard deviation (SD; ±s). Intergroup differences were assessed by one-way analysis of variance, while pairwise comparisons were conducted using the independent samples t-test (for normally distributed data with equal variance) or the rank-sum test (for non-normally distributed data). A p-value <0.05 was considered statistically significant.

RESULTS

NAC Attenuates Inflammatory Response in Rats with Pneumonia

Compared with the control group, the four groups of pneumonia model rats exhibited significantly elevated counts of EOS, LYM, and NEU in BALF (p<0.05). Among the NAC-treated groups, the low-, medium-, and high-dose groups exhibited lower EOS, LYM, and NEU counts than the model group, with the high-dose group showing the most significant reduction (p<0.05, Figure 1A). Inflammatory cytokine levels (TNF-α, IL-1β, and IL-6) followed a similar trend: the control group had the lowest levels, while the model group had the highest (p<0.05). Among the NAC-treated groups, the high-dose group demonstrated the lowest levels of

IN PRESS

TNF-α, IL-1β, and IL-6 (p<0.05, Figure B). Histopathological examination revealed intact pulmonary architecture in control animals with no inflammatory cell infiltration, whereas model group rats displayed characteristic pneumonia features including alveolar wall thickening and extensive inflammatory cell infiltration in the alveolar space. All NAC-treated groups showed improvements in lung pathology compared to the model group, with medium- and high-dose groups exhibiting the most notable reduction in inflammatory cell infiltration (Figure C).

NAC Modulates Alveolar Epithelial Cell Viability

Using CCK-8 assays, we determined the IC_{50} of NAC in A549 cells to be 3.724 (Figure 2A). Hence, we selected a concentration of 4 μmol/L for subsequent experiments. The model group cells showed significantly impaired proliferation and migration compared to the blank control group (p<0.05, Figures 2B and 2C), along with increased apoptosis (p<0.05, Figure D). NAC-treated cells showed higher proliferation and migration rates than the model group but lower than the blank control group (p<0.05, Figures 2B and 2C), while apoptosis rates were reduced compared to the model group yet remained higher than the blank control group (p<0.05) (Figure 3D).

NAC Reduced The Release Of Inflammatory Factors From Alveolar Epithelial Cells

Analysis of inflammatory factors in cell culture supernatants demonstrated significantly elevated levels of TNF-α, IL-1β, and IL-6 in the model group compared to the blank control (p<0.05). Although these cytokines remained higher in the NAC group than in the blank control group, their levels were significantly reduced compared to the model group (p<0.05) (Figure).

NAC Attenuates Ferroptosis in Alveolar Epithelial Cells

Evaluation of ferroptosis-related protein expression revealed that the model group had significantly increased levels of ACSL4, p53, and TFR1 along with decreased GPX4 and SLC7A11 compared to the blank control (p<0.05). NAC intervention partially reversed these alterations, showing: (1) significant attenuation of pro-ferroptotic proteins (ACSL4, p53, and TFR1) compared to the model group (p<0.05), though remaining elevated versus the blank control group; and (2) restoration of anti-ferroptotic factors (GPX4 and SLC7A11) to intermediate levels between pneumonia and blank control groups (p<0.05) (Figure 4).

DISCUSSION

This study systematically investigated the regulatory effects of NAC on pneumonia-related inflammatory injury and the ferroptosis process by constructing a *Klebsiella pneumoniae*-induced

IN PRESS

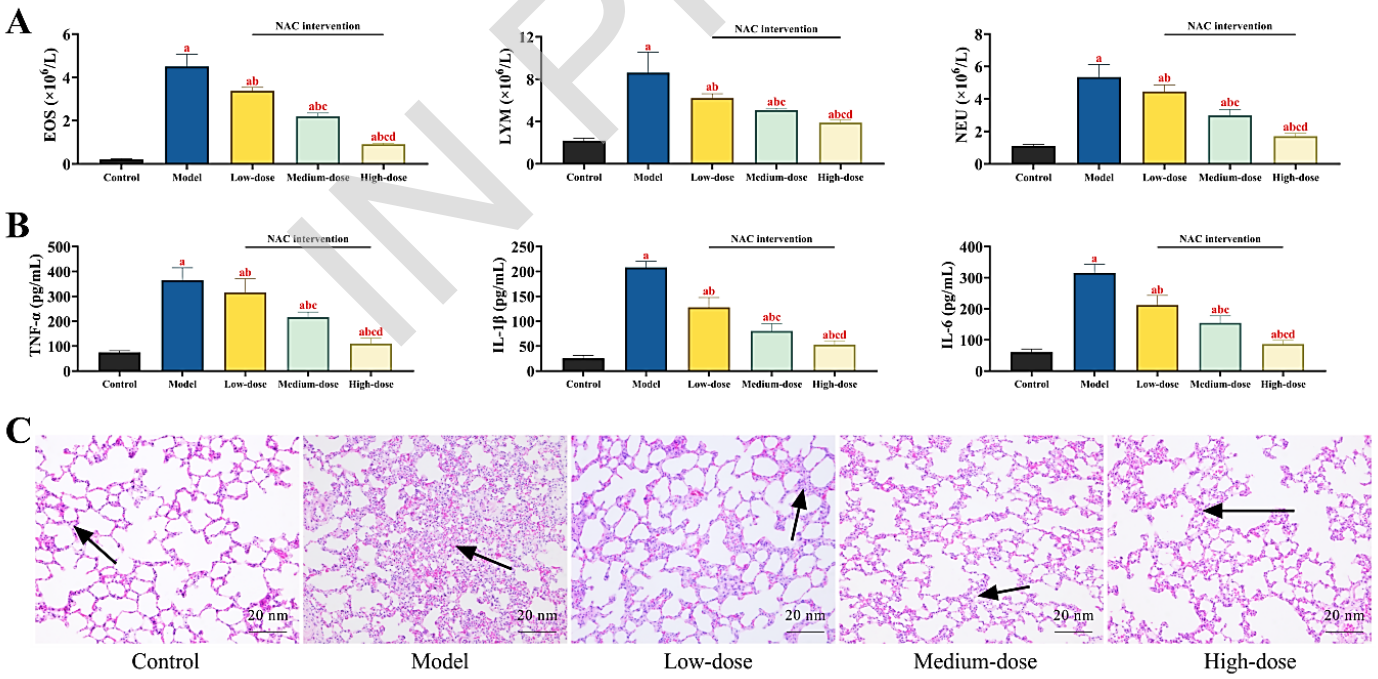


Figure 1: Effect of NAC on inflammatory cells and inflammatory factors in alveolar lavage fluid of rats with pneumonia. (A) Shows the levels of inflammatory cells EOS, LYM, NEU in alveolar lavage fluid of rats in 5 groups. (B) The levels of inflammatory factors TNF-α, IL-1β, and IL-6 in alveolar lavage fluid of rats from 5 groups were demonstrated. (C) Effect of NAC on histopathological damage of lungs of rats with pneumonia observed by HE staining (200×). Note: a indicates p<0.05 compared with the control group, b indicates p<0.05 compared with the model group, c indicates p<0.05 compared with the low-dose group, and d indicates p<0.05 compared with the medium-dose group.

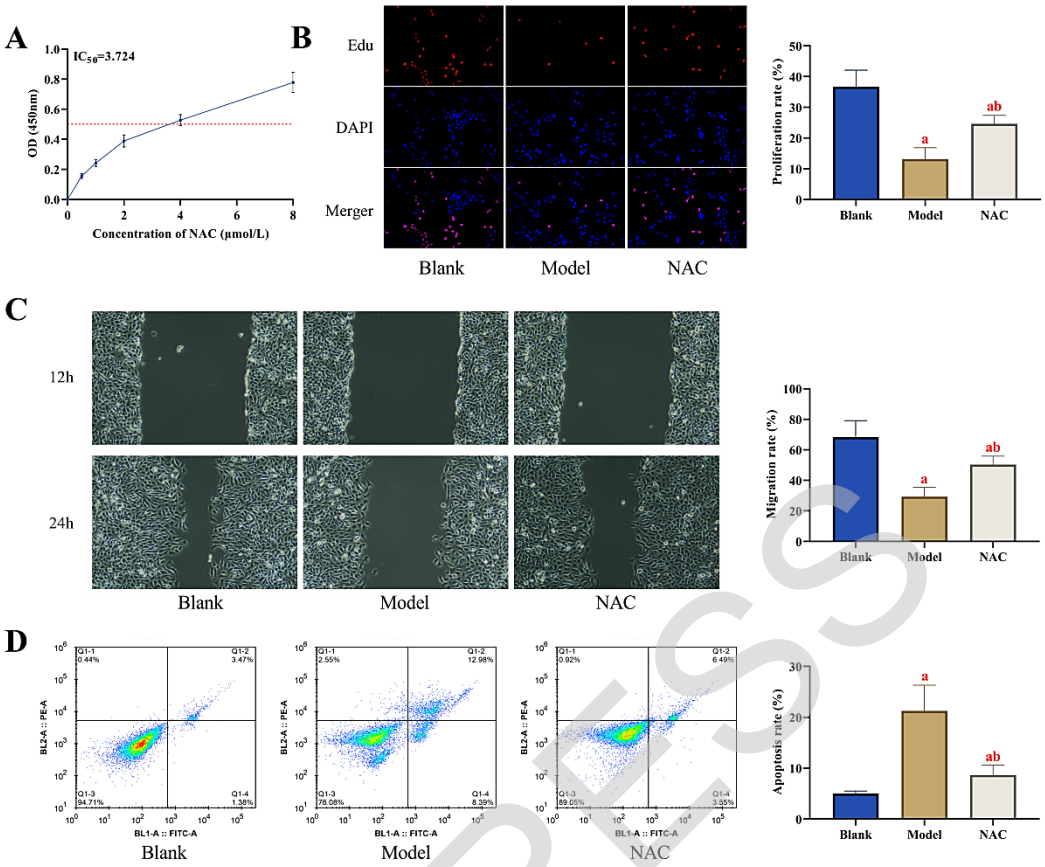


Figure 2: Effect of NAC on the activity of alveolar epithelial cells. (A) Demonstrates the IC50 of NAC in A549. (B) Demonstrates the hero of NAC on the proliferative capacity of A549 cells. (C) Demonstrated the effect of NAC on the migration ability of A549 cells. (D) Demonstrated the effect of NAC on apoptosis rate of A549 cells. Note: a indicates $p<0.05$ compared with the control group, b indicates $p<0.05$ compared with the model group, c indicates $p<0.05$ compared with the low-dose group, and d indicates $p<0.05$ compared with the medium-dose group.

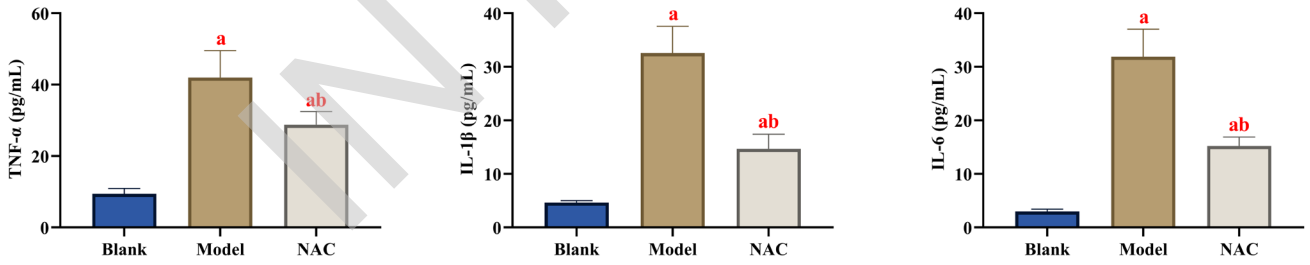


Figure 3: Effect of NAC on the levels of inflammatory factors TNF-α, IL-1β, and IL-6 in alveolar epithelial cell cultures. Note: a indicates $p<0.05$ compared with the blank group, b indicates $p<0.05$ compared with the model group.

pneumonia rat model and an LPS-stimulated inflammatory alveolar epithelial cell model. The results not only revealed the multi-target effects of NAC in inhibiting the inflammatory storm and mitigating pathological lung tissue damage but also, for the first time, clarified its key mechanism of protecting alveolar epithelial cells by intervening in the ferroptosis pathway. These findings provide a new theoretical basis for expanding the application of NAC in pneumonia treatment.

First, in *in vivo* animal experiments, we observed that NAC administration significantly attenuated inflammatory cell infiltration (EOS, LYM, and NEU) in BALF, aligning with previous reports on its anti-inflammatory efficacy in pancreatitis and pancreatic tumors.[19] We speculate that this phenomenon may be related to its inhibition of NF-κB signaling pathway activation. NAC has been shown to directly scavenge Reactive Oxygen Species (ROS) by providing sulfhydryl (-SH) groups, thereby blocking ROS-mediated nuclear translocation of NF-κB and downregulating the transcriptional expression of

IN PRESS

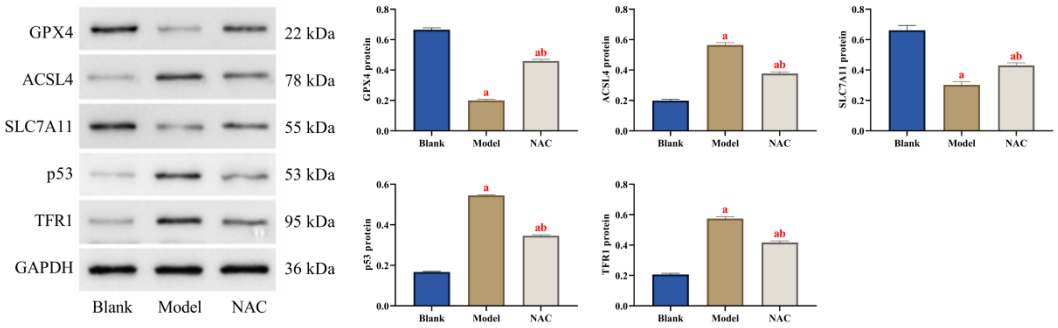


Figure 4: Effect of NAC on the expression of ferroptosis proteins ACSL4, p53, TFR1, GPX4, and SLC7A11 in alveolar epithelial cells. Note: a indicates $p<0.05$ compared with the blank group, b indicates $p<0.05$ compared with the model group.

downstream pro-inflammatory factors such as TNF-α, IL-1β, and IL-6.[20] Notably, high-dose NAC exhibited particularly significant inhibitory effects on inflammatory factors, suggesting that it may further disrupt the IL-6/JAK/STAT3 positive feedback loop by inhibiting STAT3 phosphorylation.[21] These findings are consistent with previous reports by Zhou *et al.*, regarding NAC's hepatoprotective effects, which similarly documented its potent anti-inflammatory properties in hepatic cells.[22]

In subsequent experiments utilizing the LPS-stimulated alveolar epithelial cell model, we demonstrated that NAC possesses remarkable anti-ferroptotic characteristics. At the cellular functional level, our data showed that NAC effectively reversed the LPS-induced suppression of cell proliferation while simultaneously decreasing apoptosis rates. Through wound healing assays, we further confirmed that NAC enhanced the proliferation and migration ability of epithelial cells and inhibited apoptosis, which was also consistent with the results of Wood *et al.*[23] when studying the effect of NAC on retinal cells. This finding also provides mechanistic insight into the ability of NAC to promote lung injury repair. NAC's barrier protection may derive from reduced epithelial apoptosis. Similarly, Wang *et al.*[24] also mentioned that NAC improved the barrier function of endothelial cells by inhibiting the apoptosis of endothelial cells, thus resisting the damage caused by cisplatin. Regarding ferroptosis regulation, western blot analysis clearly demonstrated that NAC enhanced the ability of cells to resist ferroptosis by activating SLC7A11 and GPX4 expression, these results provide robust experimental support for the contemporary theory proposing the GSH-GPX4 axis as the central regulatory mechanism of ferroptosis.[25] Importantly, our study represents the first experimental validation of NAC's protective effects mediated through this axis in a pneumonia model, thereby establishing a solid scientific foundation for potential clinical applications.

Several limitations of the current study warrant consideration. (1) Single pathogen model lacking viral coinfection scenarios; (2) Unmeasured oxidative markers (MDA/GSH); (3) Exclusion of female animals despite estrogen's known iron-regulatory effects. In the future, our research efforts will concentrate on two primary objectives. First, we aim to develop novel NAC nano-delivery systems designed to improve lung tissue targeting specificity and overall bioavailability. Second, we plan to employ single-cell sequencing technologies to comprehensively characterize the heterogeneous responses of alveolar epithelial cells to NAC intervention at the transcriptional level.

CONCLUSION

NAC exerts its lung-protective effects through a multidimensional mechanism involving suppression of inflammatory cytokine release, enhancement of alveolar epithelial barrier function, and inhibition of ferroptosis progression.

ACKNOWLEDGEMENT

Not applicable.

ABBREVIATIONS

ACSL4: Acyl-CoA synthetase long-chain family member 4; **BALF:** Bronchoalveolar lavage fluid; **CCK-8:** Cell Counting Kit-8; **COPD:** Chronic obstructive pulmonary disease; **EdU:** 5-Ethynyl-2'-deoxyuridine; **ELISA:** Enzyme-linked immunosorbent assay; **EOS:** Eosinophils; **FBS:** Fetal bovine serum; **FITC:** Fluorescein isothiocyanate; **GPX4:** Glutathione peroxidase 4; **GSH:** Glutathione; **H&E:** Hematoxylin and eosin; **IC_{50}:** Half-maximal inhibitory concentration; **IL-1β:** Interleukin-1 β; **IL-6:** Interleukin-6; **JAK:** Janus kinase; **LPS:** Lipopolysaccharide; **LYM:** Lymphocytes; **MDA:** Malondialdehyde; **NAC:** N-Acetylcysteine; **NEU:** Neutrophils; **NF-κB:** Nuclear factor kappa B; **NRF2:** Nuclear factor erythroid 2-related factor 2; **PI:** Propidium iodide; **PVDF:** Polyvinylidene fluoride; **ROS:** Reactive oxygen species; **SD:** Sprague-Dawley (rats); **SDS-PAGE:** Sodium dodecyl sulfate-polyacrylamide gel electrophoresis; **SLC7A11:** Solute carrier family 7 member 11; **SOD:** Superoxide dismutase; **SPF:** Specific pathogen-free; **STAT3:** Signal transducer and activator of transcription 3; **TFR1:** Transferrin receptor 1; **TNF-α:** Tumor necrosis factor-α; **ZO-1:** Zonula occludens-1.

IN PRESS

CONFLICT OF INTEREST

The authors declare that there is no conflict of interest.

FUNDING

This study was supported by the Weifang Youth Medical Talent Support Program Funding.

AVAILABILITY OF DATA AND MATERIALS

The data used to support the findings of this study are available from the corresponding author upon request.

SUMMARY

In this study, we investigated the regulatory effects and anti-inflammatory mechanisms of N-Acetylcysteine (NAC) on ferroptosis of alveolar epithelial cells in pneumonia. Using a rat model of pneumonia, it was found that a high dose of NAC (150 mg/kg) significantly reduced the levels of inflammatory cells (EOS, LYM, NEU) and cytokines (TNF-α, IL-1β, and IL-6) in alveolar lavage fluid, and attenuated the pathological damage of lung tissue. *In vitro* experiments showed that NAC (4 μmol/L) restored cell proliferation and migration capacity, reduced apoptosis, and regulated ferroptosis-related proteins. These results suggest that NAC alleviates pneumonia injury through the triple mechanism of anti-inflammation, repair of alveolar barrier and inhibition of ferroptosis.

REFERENCES

1. Hertz R, Bar-Tana J. The acylation of proteins by xenobiotic amphipathic carboxylic acids in cultured rat hepatocytes. Biochem J. 1988;254(1):39-44.
2. Sun Y, Li H, Pei Z, Wang S, Feng J, Xu L, *et al.* Incidence of community-acquired pneumonia in urban China: A national population-based study. Vaccine. 2020;38(52):8362-70.
3. Todkill D, Lamagni T, Pebody R, Ramsay M, Woolham D, Demirjian A, *et al.* Persistent elevation in incidence of pneumonia in children in England, 2023/24. Euro Surveill. 2024;29(32).
4. Ai J, Zhu Y, Duan Y, Zhang M, Lu G, Sun Y, *et al.* A multicenter study on molecular epidemiology of rhinovirus isolated from children with community acquired pneumonia in China during 2017-2019. Infect Genet Evol. 2022;106:105384.
5. Huang Z, Chen K, Yang X, Cui H, Wu Y, Wang Y, *et al.* Spatial metabolomics reveal mechanisms of dexamethasone against pediatric pneumonia. J Pharm Biomed Anal. 2023;229:115369.
6. Feng F, He S, Li X, He J, Luo L. Mitochondria-mediated Ferroptosis in Diseases Therapy: From Molecular Mechanisms to Implications. Aging Dis. 2024;15(2):714-38.
7. Wu D, Spencer CB, Ortoga L, Zhang H, Miao C. Histone lactylation-regulated METTL3 promotes ferroptosis via m6A-modification on ACSL4 in sepsis-associated lung injury. Redox Biol. 2024;74:103194.
8. Shen M, You Y, Xu C, Chen Z. Epigallocatechin-3-Gallate attenuates lipopolysacharide-induced pneumonia via modification of inflammation, oxidative stress, apoptosis, and autophagy. BMC Complement Med Ther. 2024;24(1):147.
9. Papi A, Alfano F, Bigoni T, Mancini L, Mawass A, Baraldi F, *et al.* N-acetylcysteine Treatment in Chronic Obstructive Pulmonary Disease (COPD) and Chronic Bronchitis/ Pre-COPD: Distinct Meta-analyses. Arch Bronconeumol. 2024;60(5):269-78.
10. Hu M, Zhang Y, Ma S, Li J, Wang X, Liang M, *et al.* Suppression of uterine and placental ferroptosis by N-acetylcysteine in a rat model of polycystic ovary syndrome. Mol Hum Reprod. 2021;27(12).
11. Zhou D, Yang Y, Chen J, Zhou J, He J, Liu D, *et al.* N-acetylcysteine Protects Against Myocardial Ischemia-Reperfusion Injury Through Anti-ferroptosis in Type 1 Diabetic Mice. Cardiovasc Toxicol. 2024;24(5):481-98.
12. Wang R, Gan C, Mao R, Chen Y, Yan R, Li G, *et al.* Rat models of postintracerebral hemorrhage pneumonia induced by nasal inoculation with Klebsiella pneumoniae or intratracheal inoculation with LPS. Front Immunol. 2024;15:1477902.
13. Jia J, Yuan Y, He Y, Wasti B, Duan W, Chen Z, *et al.* Inhibition of METTL3 alleviated LPS-induced alveolar epithelial cell apoptosis and acute lung injury via restoring neprilysin expression. Life Sci. 2023;333:122148.
14. Minati MA, Libert M, Dahou H, Jacquemin P, Assi M. N-Acetylcysteine Reduces the Pro-Oxidant and Inflammatory Responses during Pancreatitis and Pancreas Tumorigenesis. Antioxidants (Basel). 2021;10(7).
15. Wang J, Zhang C, Zhao R, Wang P, Jin M, Xu J. Antioxidant N-acetylcysteine removing ROS: an antifouling strategy inspired by mussels. Environ Sci Process Impacts. 2023;25(12):1962-73.
16. Zhao M, Wen Y, Yang Y, Pan H, Xie S, Shen C, *et al.* (-)-Asarinin alleviates gastric precancerous lesions by promoting mitochondrial ROS accumulation and inhibiting the STAT3 signaling pathway. Phytomedicine. 2024;126:155348.
17. Li Y, Guo M, Wang Q, Zhou H, Wu W, Lin H, *et al. Glaesserella parasuis* serotype 5 induces pyroptosis via the RIG-I/MAVS/NLRP3 pathway in swine tracheal epithelial cells. Vet Microbiol. 2024;294:110127.
18. Dong G, Li Q, Yu C, Wang Q, Zuo D, Li X. n-Acetylcysteine protects against diazinon-induced histopathological damage and apoptosis in renal tissue of rats. Toxicol Res. 2024;40(2):285-95.
19. Zhou WT, Wang LB, Yu H, Zhang KK, Chen LJ, Wang Q, *et al.* N-acetylcysteine alleviates PCB52-induced hepatotoxicity by repressing oxidative stress and inflammatory responses. PeerJ. 2020;8:e9720.
20. Wang X, Shen T, Lian J, Deng K, Qu C, Li E, *et al.* Resveratrol reduces ROS-induced ferroptosis by activating SIRT3 and compensating the GSH/GPX4 pathway. Mol Med. 2023;29(1):137.

Cite this article: Zhao X, Wang X, Zhao T. N-Acetylcysteine in Pneumonia: Modulatory Effects on Pulmonary Inflammation and Alveolar Epithelial Cell Ferroptosis. Indian J of Pharmaceutical Education and Research. 2026;60:10.5530/ijper.20262558.

IN PRESS